HHS Public Access

Author manuscript

ACS Biomater Sci Eng. Author manuscript; available in PMC 2021 November 27.

Published in final edited form as:

ACS Biomater Sci Eng. 2019 March 11; 5(3): 1332–1342. doi:10.1021/acsbiomaterials.8b01591.

Pentablock Copolymer Micelle Nanoadjuvants Enhance Cytosolic Delivery of Antigen and Improve Vaccine Efficacy while Inducing Low Inflammation

Sujata Senapati[†,‖], **Ross J. Darling**[‡,‖], **Darren Loh**[§], **Ian C. Schneider**[†,‖], **Michael J. Wannemuehler**[‡,‖], **Balaji Narasimhan**[*,†,‖], **Surya K. Mallapragada**[*,†,‖]

[†]Department of Chemical and Biological Engineering, Iowa State University, Ames, Iowa 50011, United States

[‡]Department of Veterinary Microbiology and Preventive Medicine, Iowa State University, Ames, Iowa 50011, United States

[§]Department of Chemical and Biological Engineering, Johns Hopkins University, Baltimore, Maryland 21218, United States

[‖]Nanovaccine Institute, Iowa State University, Ames, Iowa 50011, United States

Abstract

As the focus has shifted from traditional killed or live, attenuated vaccines toward subunit vaccines, improvements in vaccine safety have been confronted with low immunogenicity of protein antigens. This issue has been addressed by synthesizing and designing a wide variety of antigen carriers and adjuvants, such as Toll-like receptor agonists (e.g., MPLA, CpG). Studies have focused on optimizing adjuvants for improved cellular trafficking, cytosolic availability, and improved antigen presentation. In this work, we describe the design of novel amphiphilic pentablock copolymer (PBC) adjuvants that exhibit high biocompatibility and reversible pH- and temperature-sensitive micelle formation. We demonstrate improved humoral immunity in mice in response to single-dose immunization with PBC micelle adjuvants compared with soluble antigen alone. With the motive of exploring the mechanism of action of these PBC micelles, we studied intracellular trafficking of these PBC micelles with a model antigen and demonstrated that the PBC micelles associate with the antigen and enhance its cytosolic delivery to antigen-presenting cells. We posit that these PBC micelles operate via immune-enhancing mechanisms that are different from that of traditional Toll-like receptor activating adjuvants. The metabolic profile of antigen-presenting cells stimulated with traditional adjuvants and the PBC micelles also suggests

[*]**Corresponding Authors**: suryakm@iastate.edu, nbalaji@iastate.edu.

The authors declare no competing financial interest.

ASSOCIATED CONTENT

Supporting Information

The Supporting Information is available free of charge on the ACS Publications website at DOI: 10.1021/acsbiomaterials.8b01591. Mean fluorescence intensity (MFI) of micelle-positive BMDCs and J774 cells, trafficking of antigen into BMDCs and J774 cells, time-course of the ovalbumin uptake when incubated with pentablock copolymer (PBC) micelles for BMDCs and J774 cells, data demonstrating that pentablock copolymer (PBC) micelles did not show significant upregulation of costimulatory molecules in bone marrow macrophages and did not induce pro-inflammatory cytokine secretion, and data showing that PBC micelle adjuvants do not induce nitric oxide in J774 cells and bone marrow macrophages (PDF)

distinct mechanisms of action. A key finding from this study is the low production of nitric oxide and reactive oxygen species by antigen-presenting cells when stimulated by PBC micelle adjuvants in sharp contrast to TLR adjuvants. Together, these studies provide a basis for rationally developing novel vaccine adjuvants that are safe, that induce low inflammation, and that can efficiently deliver antigen to the cytosol.

Graphical Abstract

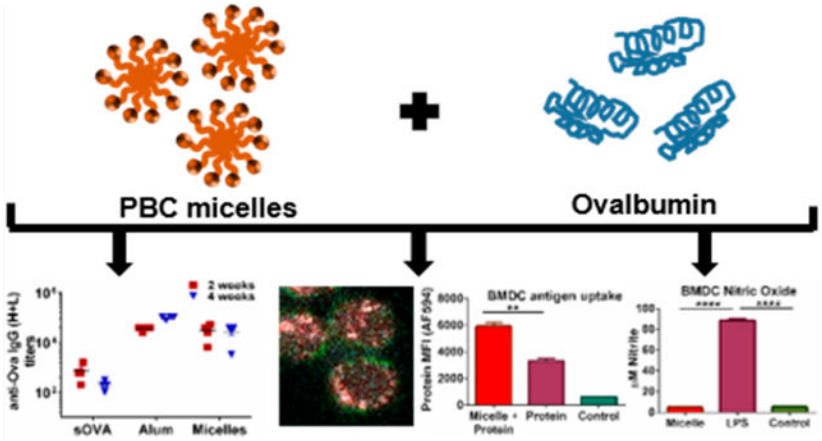

Keywords

adjuvant; micelles; block copolymers; antigen delivery; antibody-mediated immunity; immunometabolism

INTRODUCTION

Adjuvants have been used for almost seven decades to augment immune responses to antigens in subunit vaccines.[1–4] However, only a few, such as alum and monophosphoryl lipid A (MPLA), are currently approved by the United States Food and Drug Administration for use in human vaccines.[5] These adjuvants suffer from several limitations, including high reactogenicity, failure to provide cell-mediated immunity, and variability in the induction of immune responses in older adults.[6–8] Most vaccines or adjuvants that are currently approved or in preclinical trials work by the stimulation of pathogen recognition receptors (PRRs) on antigen-presenting cells (APCs). This leads to the induction of inflammatory signals, such as cytokines, superoxides, and nitric oxide (NO).[5] However, because of immunosenescence in older adults, this cytokine milieu is highly imbalanced leading to a state of “inflamm-aging” and an overproduction of harmful oxide analytes.[9,10] While the traditional approach for vaccine design works in most cases, the presence of inflammaging in older adults necessitates the development (and exploration of mechanism of action) of novel vaccine adjuvants that do not induce the production of harmful analytes while stimulating the immune system.

A significant amount of research has been focused on improving transport and delivery of antigens and adjuvants to APCs.[11,12] These antigens can be processed by APCs and

presented via MHC I or MHC II pathway for the induction of effective T and B cell responses.[12] Studies have focused on pH-sensitive amphiphilic polymer-based vaccine delivery vehicles to enhance antigen presentation to the MHC I pathway and to induce $CD8^+$ T cell responses that can be beneficial for enhancing the breadth of protection against intracellular pathogens.[13–15] In particular, cationic polymeric systems have been shown to enhance endosomal escape of the antigen due to the proton sponge effect and enhance cytosolic uptake of the antigen.[16–18]

Amphiphilic pentablock copolymers based on Pluronic F127, poly(ethylene oxide) (PEO) and poly(propylene oxide) (PPO), and cationic blocks such as poly(diethylaminoethyl methacrylate) (PDEAEM) have been previously studied for drug delivery and gene delivery.[19–21] Aqueous solutions of these polymers can form spherical micelles (about 30 nm in diameter) and at higher concentrations (>20 wt % polymer) form physical hydrogels in response to both temperature and pH.[22,23] The observation that small particle sizes of antigen delivery systems can enhance internalization by APCs has been widely exploited by different nanoparticle systems.[24–27] Therefore, a polymer system having both sub-100 nm size and stimuli responsiveness can be extremely beneficial. Hydrogels based on these pentablock copolymers (PBC) have been shown to provide sustained release of structurally stable antigen in vivo and enhance antiovalbumin (Ova) antibody responses.[28,29] We have also demonstrated in previous influenza virus challenge experiments that these PBC formulations can enhance neutralizing antibody titers that effected a reduction in viral load in lungs and exhibit improved vaccine efficacy in mice.[30] In this study, we prepared low concentration PBCs in aqueous solutions to form micelles without gelation that still enhanced antibody responses. This also eliminates any potential inflammatory responses associated with the high polymer concentrations needed to form gels.[31] However, little is known about the mechanism of action of PBC micelle adjuvants; how they interact with innate immune cells; and how these interactions lead to the induction of effective adaptive immunity.

In this work, to explore the mechanism of action of these PBC micelles, we characterized antigen–micelle complexes using Forster Resonance Energy Transfer (FRET) spectroscopy and microscopy and showed that Ova associated with the micelles in the solution phase and that the PBC micelles enhanced Ova delivery to the cytosol in vitro in APCs. We also studied the stimulation of APCs with antigen-containing PBC micelles using three different approaches. In the first phase, we analyzed the upregulation of costimulatory molecules and cytokine secretion profile from APCs. Next, we measured the oxygen consumption rate by the mitochondria of APCs as a measure of stimulation. We analyzed the mitochondrial respiration and metabolic profile in comparison to the TLR agonist lipopolysaccharide (LPS). Finally, we studied the amount of innate effector molecule (such as NO and reactive oxygen species (ROS)) secretion by APCs upon stimulation with PBC micelles. Collectively, the studies presented here focus on the analysis of the responses of innate immune cells stimulated by novel PBC micelle adjuvants in order to understand their mechanism of action so as to develop safe and effective adjuvants with low inflammatory potential.

EXPERIMENTAL SECTION

Materials.

N,N-(Diethylamino)ethyl methacrylate (DEAEM), Pluronic F127, Poly(vinyl alcohol) (PVA, MW = 9000–10 000 g/mol), and ovalbumin (Ova, 44 kDa) were purchased from Sigma-Aldrich (St. Louis, MO). Alum (Alhydrogel) and dyes for imaging and labeling were purchased from InVivogen (San Diego, CA). All other materials were purchased from Fisher Scientific (Pittsburgh, PA).

Methods.

Pentablock Copolymer Synthesis and Characterization.—Pentablock copolymer (PDEAEM–PEO-PPO–PEO-PDEAEM) was synthesized by atom transfer radical polymerization (ATRP) as reported previously.[22] This method utilizes a difunctional macroinitiator prepared from commercially available Pluronic F127. This was dissolved in tetrahydrofuran and reacted overnight with triethylamine and 2-bromoisobutyryl. The product was precipitated in *n*-hexane. The 2-bromo propionate Pluronic F127 was analyzed using ^{1}H NMR to confirm the end group functionalization. Next, the macroinitiator and the monomer DEAEM were used to synthesize the pentablock copolymer by ATRP utilizing copper(I) oxide nanoparticles as the catalyst and N-propylpyrilidinemethanamine (NPPM) as the complexing ligand. Cuprous oxide nanoparticles used as catalyst were synthesized as previously described.[32] ^{1}H NMR spectra of the resulting polymer were used to determine molecular weight.

Labeling of PBC and Antigen with Fluorescent Dyes.—The PBC and Ova were labeled with dyes to detect them fluorescently. We utilized an Alexa Fluor 594 protein labeling kit that utilizes a succinimidyl ester moiety to react with the primary amines of the proteins (Molecular Probes, Eugene, OR) for labeling ovalbumin according to the manufacturer's protocol. For labeling the PBC, we functionalized the end groups with azide following a previously described protocol.[28] We then utilized azide–alkyne click chemistry to attach alkyne functionalized Alexa Fluor 647 (Thermo Fisher Scientific, Waltham, MA) according to the manufacturer's protocol.

PBC Hydrogel and Micelle Formulations.—A stock solution of 30% PVA was prepared in phosphate-buffered saline (PBS). For the hydrogel formulation, this stock solution was added to obtain a final concentration of 15 wt % PVA, 5.9 wt % Pluronic F127 and 4.1 wt % PBC in PBS. For the micelle formulation, a similar procedure was followed to obtain a final concentration of 7.5 wt % PVA, 2.95 wt % Pluronic F127 and 2.05 wt % PBC in PBS. A micelle formulation with the fluorescently labeled PBC was also prepared and used in experiments as required.

Animals.—Female C57BL/6 or BALB/c mice (6–7-week-old) were purchased from Charles River Laboratories (Wilmington, MA). The Institutional Animal Care and Use Committee (IACUC) at Iowa State University approved all protocols involving animals.

Immunizations and Evaluation of Antibody Titers.—To evaluate antibody responses, C57BL/6 or BALB/c mice were subcutaneously immunized with 100 μL of the micelle formulation, 100 μL of hydrogel formulation, or alum in a 1:1 ratio with Ova, all containing 50 μg of Ova. Control animals were immunized with soluble Ova in PBS (50 μg in 100 μL) (i.e., no adjuvant). Serum samples were collected via the saphenous vein at 21 days and 35 days postimmunization. Enzyme-linked immunosorbent assay (ELISA) was performed to measure the total anti-Ova total IgG titers. Briefly, high binding 96-well ELISA plates were coated with Ova overnight and blocked with 2% w/v gelatin (BD Difco, Fisher Scientific, Hampton, NH) in 0.05% Tween-PBS solution the following day. Serum samples were added at a dilution of 1:200 and diluted 1:2 across the plate. After incubation and washing, alkaline-phosphatase-conjugated antimouse IgG (H+L) (Jackson ImmunoResearch, Westgrove, PA) was added and incubated for 2 h before adding substrate buffer and reading the plate at 405 nm. Titer was recorded as the last dilution that exhibited an optical density greater than twice the background optical density.

Generation of Bone Marrow Dendritic Cells (BMDCs) and Bone Marrow Macrophages (BMMs).—Bone marrow was harvested from femurs and tibia of BALB/c mice and differentiated to dendritic cells using a standard protocol.[33] Briefly, the bone marrow was flushed out of the bones using a syringe with 5 mL of RPMI media containing 1% (1 g/100 mL) pen/strep. Granulocyte macrophage colony stimulating factor (GM-CSF) was added on the first day of culture at the concentration of 1 ng/mL. GM-CSF and medium was refreshed on days 3, 6, and 8 of culture by exchanging 10 mL of spent medium with fresh medium containing GM-CSF. BMDCs were harvested on day 10 and used in subsequent assays. The same protocol was followed for BMMs except using DMEM medium and macrophage colony stimulating factor (M-CSF) as the cytokine at a concentration of 1 ng/mL.

Confocal Microscopy.—J774 macrophage cell line and BALB/c-derived BMDCs were used to analyze the cellular internalization of antigen-containing micelles using confocal microscopy. Cells were cultured on and allowed to adhere to round glass coverslips (VWR, Radnor, PA) in 24 well flat-bottom cell culture plates overnight. For J774s, since they are adherent, no coating on the coverslips was used. However, for the BMDCs we treated the coverslips with poly D-lysine for 12 h before cell culture. The cells were incubated for 15 min, 30 min, 2 and 12 h with the labeled Ova solution (20 μg/mL) and the micelle formulation (12.5 μg/mL) consisting of labeled PBC, together and separately as controls. For the groups treated with micelle-Ova complex, the micelle and Ova solutions were coincubated for an hour before adding them to the cells. The cells were then stained with Hoescht 33342 solution for nuclear staining (ThermoFisher Scientific) as described in the commercial protocol. Antimouse LAMP-1 (1D4B) (Developmental Studies Hybridoma Bank, University of Iowa) was used to stain lysosomes in BMDCs. The cells were then fixed and the coverslips were mounted on microscopic slides (VWR, Radnor, PA). A Leica SB5 X MP confocal microscope was used to image the cell samples, and the images were analyzed using LAS AF software (Leica Microsystems, Wetzlar, Germany).

FRET Spectroscopy and Microscopy.—AF594 tagged to Ova and AF647 tagged to the PBC (Forster radius, R_0 = 8.5 nm) acted as the donor and acceptor fluorophore, respectively, for FRET analysis. Solutions with 12.5 μg/mL of PBC micelle formulation and 20 μg/mL of Ova were mixed together or added separately to measure the fluorescence spectra using a dual monochromator spectrofluorometer (Fluoromax-4, Horiba Jobin Yvon, Kyoto, Japan) with a slit width of 3 nm at the excitation of the donor (590 nm) and emission wavelengths for the two fluorophores (AF594 Em: 610 nm and AF647 Em: 660 nm).

For FRET microscopy, a Leica SB5 X MP confocal microscope was used for slides prepared in a similar manner as confocal microscopic imaging using the same concentrations of the PBC micelle and Ova solutions. However, the settings in the microscope were changed according to the procedure used to measure sensitized emission for FRET,[34] which involves the measurement of acceptor emission change with the addition of the donor. The different images taken in order were the following: (a) FRET sample images in the FRET channel (donor excitation and acceptor emission), donor channel (donor excitation and donor emission), acceptor channel (acceptor excitation and acceptor emission); (b) Acceptor only sample image in the acceptor channel; and (c) Donor only sample image in the donor channel. The last two images were taken to correct for the spectral bleed-throughs in the channel to subtract the amount of radiation detected in the FRET channel, which is not due to the energy transfer. The instrument settings were kept constant throughout the imaging. The bleed-through was calculated using a linear regression obtained by the FRET and colocalization analyzer plugin in ImageJ software (NIH, Bethesda, MD). Final FRET index images, heat maps in the “fire” Look-Up Table (LUT) and mean FRET indices were generated by selecting regions of interest (ROIs) in the images where cells were present.

In Vitro APC Stimulation.—BALB/c-derived BMDCs, BMMs, and J774s were plated at 5×10^5 cells/well in a 96-well round-bottom tissue culture plate in 200 μL of complete RPMI 1640 medium with 1% pen/strep (1 g/100 mL). Stimulations were carried out overnight or for 48 h using 12.5 μg/mL of micelles, 1 μg/mL of LPS, or untreated control wells. Supernatants were collected for cytokine analysis and NO quantification, and cells were harvested (using cell scrapers for BMMs and J774s) for cell surface maker expression and mitochondrial and cell superoxide production by flow cytometry.

Cytokine Secretion Assay.—The cell-free supernatants collected after stimulating the different cellular populations for 48 h were used to evaluate the levels of cytokine secretions. BioRad BioPlex 200 system (Hercules, CA) was used to analyze IL-6, TNF-α, IL-1β, IL-12, and IFNγ secretions.

Flow Cytometry.—Costimulatory marker expression on APCs was evaluated using flow cytometry. BMDCs at a concentration of 5×10^5 cells/200 μL were aspirated from a 96-well plate and transferred to polystyrene FACS tubes. Prior to labeling with specific monoclonal antibodies, Fc receptors on DCs were blocked to prevent nonspecific antibody binding by incubating the cells with 100 μg/mL of rat IgG (Sigma-Aldrich, St. Louis, MO) and 10 μg/mL of anti-CD16/32 (eBioscience). Subsequently, APCs were stained with fluorescently conjugated antibodies for CD80 (Biolegend, PerCP-Cy5.5, clone 16–10A1), CD86 (eBioscience, FITC, clone GL1), CD40 (eBioscience, APC, clone 1C10), CD11c

(Biolegend, APC-Cy7, clone N418), MHCII (eBioscience, AF700, clone M5/114.15.2) diluted at 1:50 v/v in FACS buffer.

Mitochondrial superoxide production was evaluated using live cells stained with MitoSOX Red (ThermoFisher Scientific) according to manufacturer's specifications. The amount of reactive oxygen species (ROS) produced by the BMDCs was measured using CellROX Green (ThermoFisher Scientific) according to the manufacturer's protocol.

Fluorescent activated cell sorting (FACS) was used to quantify the internalization of protein and micelles into BMDCs and a macrophage cell line J774. The cells were treated with either the labeled Ova (20 μg/mL) or the PBC micelles (12.5 μg/mL), or the micelle-Ova complex obtained after an hour of incubation of the solutions, for multiple time intervals (15 min, 30 min, 2 h and 12 h). After the incubation, the cells were transferred to FACS tubes and suspended and washed in FACS buffer to remove the excess dye not taken up by the cells. All the samples for flow cytometry except the MItoSOX and CellROX samples were fixed using BD stabilizing fixative (BD Bioscience, Franklin Lakes, NJ). Data was collected on a FACSCanto II (BD Bioscience, Franklin Lakes, NJ), and analyzed using FlowJo (Flowjo LLC, Ashland, OR).

Extracellular Flux Analysis.—Metabolic effect of stimulation of BMDCs was measured using two assays. For measurement of oxidative phosphorylation, the oxygen consumption rate (OCR) was analyzed by performing an overnight stimulation of BMDCs with either 12.5 μg/mL of PBC micelles, 1 μg/mL of LPS, or untreated control, was carried out in 5 mL polypropylene tubes. 2.5×10^5 stimulated BMDCs were seeded into Cell-Tak (Corning, Corning NY) coated Seahorse plates and a mitochondrial stress test (MST) was conducted according to manufacturer's specifications using kit concentrations of 1 μM oligomycin, 2 μM FCCP, and 0.5 μM rotenone and antimycin (Agilent, Santa Clara, CA).

For measurement of acute metabolic responses and glycolysis (demonstrated by extracellular acidification rate, ECAR) upon stimulation, untreated BMDCs were seeded into Cell-Tak (Corning, Corning NY) coated seahorse plates at a density of 2.5×10^5 untreated BMDCs per well. Baseline metabolic activity readings were measured, and wells were stimulated with 12.5 μg/mL of micelle, 1 μg/mL of LPS, or medium control, and metabolic measurements are taken over the course of the assay. All metabolic phenotyping was conducted on a Seahorse XFe24 (Agilent, Santa Clara, CA).

Nitric Oxide Quantification.—Nitric oxide (NO) in supernatants obtained from BMDCs, BMMs, and J774 cells after stimulation for 48 h was quantified using a Griess assay. A sodium nitrite standard curve was created with concentrations ranging from 100 μM to 0 μM. One hundred microliters of Griess reagent (cat. no. 03553, Sigma-Aldrich) was added to 100 μL of standard or sample supernatant in a 96-well microtiter plate. Samples were allowed to react for 15 min at room temperature and read at 540 nm on a SpectraMAX 190 (Molecular Devices, Sunnyvale, CA) plate reader. Experimental nitrite concentrations were calculated using a linear regression method.

Statistics.—For the antibody titer data, statistical significance was determined using one-way ANOVA and Tukey-post *t* test on the log 2 transformed titers using GraphPad (Prism 7.0, GraphPad Software, La Jolla, CA). For all other experiments, statistical significance was determined using one-way ANOVA analysis of the respective values using GraphPad, and *p*-values ≤0.05 were considered significant.

Results.

PBC Micelle Nanoadjuvant Enhances Antibody-Mediated Immunity.—The ATRP method yielded PBC with outer cationic PDEAEM blocks having a molecular weight of 14 680 g/mol as determined by ^{1}H NMR. The micelle formulation prepared from PBC was administered to mice with Ova to evaluate the induction of humoral immune responses. In addition, separate groups of mice were administered either soluble ovalbumin (sOVA), alum+Ova or a hydrogel formulation (as used in previous studies), all containing 50 μg of Ova.[29] We observed a 9-fold increase in anti-Ova antibody titers in sera of mice immunized with micelles when compared with sOVA at 2 weeks postimmunization (p.i.) (Figure 1).

This fold-increase was sustained through 4 weeks p.i. In addition, we observed a significant increase in anti-OVA antibody titers in sera of animals immunized with the hydrogel formulation over the sOVA, consistent with our previous studies.[29] However, there were no significant differences observed between the micelle and hydrogel formulations, indicating that the PBC micelle enhanced humoral immunity even at much lower polymer concentration (compared with the hydrogel formulation). This suggests that the thermogelation or depot formation of the PBC hydrogel at the site of injection is not the only mechanism of action of this adjuvant. We also observed that the antibody titers in the animals immunized with alum+Ova, which were not significantly different from the titers induced in the animals immunized with PBC micelles at 2 weeks p.i., became significantly different (about 4-fold higher) at 4 weeks p.i. We also performed anti-Ova IgM titers (data not shown) that showed similar trends as IgG.

PBC Micelle Nanoadjuvants Exhibit Cytosolic Uptake of Antigen by BMDCs and J774 Cells.—To understand the mechanism of action of these PBC micelles and identify factors that may contribute to the enhancement in humoral immunity when immunized with micelles, we decided to first probe their interaction with the APCs. Internalization of proteins or peptides by the APCs is the first step in the triggering of immune signaling to generate an immune response.[35,36] We studied the internalization of OVA-containing micelles by BMDCs and J774 cells using confocal microscopy. We observed that the micelles (cyan) and ovalbumin (red) were internalized efficiently by both the cell types into the cytosol after a 30 min incubation time and stayed the same until the 12-h incubation time (Figure 2, SI Figure 2). However, we did not observe any internalization at the 15 min time point (SI Figure 2). After 12 h of incubation, we could observe antigen in BMDCs colocalized with the lysosomes (shown in green, Figure 2A). However, most of the antigen was distributed across the cytosol indicating antigen release from the micelles. In addition, because of their amphiphilic nature, we also observed a large amount of micelles interacting with the cell membrane, especially in the J774 cells starting at 15 min until after 12 h of incubation. We also analyzed the cells that had incorporated

micelles using FACS. Almost 100% of the BMDCs and J774 cells were positive for the micelles as soon as 15 min and the labeling remained stable for at least 12 h as indicated by the clear shifts in the population in the flow cytometry plots (SI Figure 1). The mean fluorescence intensity (MFI) of the micelle-positive cell population, however, increased from 15 min to 12 h for both BMDCs and J774 cells.

PBC Micelle Nanoadjuvants Associate with Antigen and Enhance Their Uptake.—Next, we assessed the nature of interaction of the PBC micelles with the antigen using FRET. We first incubated micelles with Ova labeled with dyes that exhibit FRET in solution phase for 15 min and studied the fluorescence spectrum of three solutions: (a) micelles only, (b) Ova only, and (c) micelles + Ova. FRET occurs if the donor and acceptor fluorophores are spatially proximal (less than 10 nm).[37] Upon occurrence of FRET, we observed a decrease in the intensity of donor fluorescence (at 610 nm for the dye tagged with ovalbumin) and an increase of almost the same magnitude in the acceptor intensity (at 660 nm the dye tagged with the micelles) when both were in solution together, compared to when they were in solution separately (Figure 3). These observations showed that the micelles associate with the antigen in solution phase.

We then evaluated whether the same phenomenon occurs in the presence of immune cells. We incubated J774 cells and BMDCs with micelles and Ova at different concentrations overnight and included micelles-only and Ova-only controls. After removal of spectral bleed-throughs and analysis of the images as described in the Methods section, we obtained mean FRET indices. We observed the highest FRET indices for a polymer concentration of 12.5 μg/mL and protein concentration of 25 μg/mL (mean FRET index = 16.8 for BMDCs and = 9.6 for J774 cells, generated using the histograms) as shown in Figures 4A and 4B. The images generated by the FRET analyzer plugin provided us with an estimate of the degree of FRET occurring.[34] We observed greater FRET (as indicated by the color in the images and the heat map) in BMDCs than in J774 cells. We also observed some areas of very high FRET in both cell types (indicated by magenta color in the images).

We hypothesized that the association of the micelles with antigen may assist the antigen being carried into the cytosol. Therefore, we performed FACS with J774 cells and BMDCs stimulated with micelles and ovalbumin at the same concentration at which we observed the highest FRET. We observed about a 2-fold increase in the antigen mean fluorescence intensity (MFI) when the BMDCs were incubated with both the micelles and antigen than with the antigen alone after 12 h of incubation (Figure 4C). The amount of antigen delivered to the cells also increased from 15 min to 12 h of incubation, and we observed significantly more antigen at the 1 and 2 h incubation periods for BMDCs than after 15 or 30 min of incubation. (SI Figure 3). We observed a slight (although not significant) increase in antigen MFI when J774 cells were used.

APC Stimulation by PBC Micelle Nanoadjuvants.—While these previous experiments provided us valuable information about micelleantigen interactions, an understanding of how immune cells perceive the antigen when it is adjuvanted with micelles is necessary. The activation of APCs such as DCs is an important part of the induction of innate and adaptive immune responses. DCs are activated by recognition of

damage-associated molecular patterns (DAMPs) or microbial-associated molecular patterns (MAMPs), and they undergo maturation and upregulate different cell surface markers.[38,39] To characterize the same, we assessed the expression of CD40, CD80, CD86 and MHCII in BMDCs and BMMs using flow cytometry when stimulated with PBC micelles for 48 h. Overall, we observed little to no significant upregulation of these markers in BMDCs (Figure 5) or BMMs (SI Figure 4) with PBC micelles, compared to negative controls. However, the positive control, LPS, induced significantly higher levels of these surface markers, consistent with the literature.[40]

We also analyzed the levels of different cytokine secretions by the APCs. The cytokine milieu often determines the fate of various immune responses. We did not observe any secretion of the pro-inflammatory cytokines, IL-6, TNF-α, IL-1β, IL-12, IFNγ from BMDCs and BMMs (Figure 5, SI Figure 4 and data not shown) in response to the PBC micelle formulations. We observed very high levels of pro-inflammatory cytokines secreted by APCs stimulated with LPS (Figure 5 and SI Figure 2). Altogether, these data demonstrate the low APC-stimulating characteristics of the PBC micelles unlike traditional TLR-agonist adjuvants, such as LPS.

Immunometabolic Profile of PBC Micelle Nanoadjuvants.—Recent advances in the field of immunometabolism have described the relationship between DC activation and the corresponding metabolic changes.[41–43] Several hours postexposure to TLR ligands, BMDCs exhibit a dramatic shift to a dependence on aerobic glycolysis for survival and generation of ATP.[44] This effect is driven by the nitrosylation of electron transport chain (ETC) molecules after production of large amounts of NO as a result of encounter with TLR ligands.[45] As a result, BMDCs exhibit a distinct immediate glycolytic burst upon activation with TLR ligands. This provides a rapid and sensitive method to detect whether BMDCs were actively recognizing and responding to a particular adjuvant formulation.[46] Resting BMDCs were measured for baseline glycolytic activity and then exposed to LPS, PBC micelle, or medium control. Medium acidification rates were recorded as a measure of glycolytic activity. Immediately upon exposure to LPS, BMDCs exhibited an increase in glycolytic rate, while exposure to the micelle formulation showed levels of glycolysis similar to the control over the course of the assay (Figure 6A).

To evaluate the metabolic consequences of exposure of BMDCs to PBC micelles, we probed mitochondrial respiratory function with a mitochondrial stress test (Figure 6B). Several parameters, such as basal respiration, ATP production, maximum respiration, and spare capacity were measured using sequential injections of different drugs.[47] Addition of oligomycin, an inhibitor of ATP synthase, complex V, provided the ATP production rate. The addition of FCCP, which is a protonophore drives the ETC to function at its maximal rate, provided the maximal and spare respiratory capacity of the cells. Addition of rotenone, which shuts down the ETC provided the rate of nonmitochondrial respiration to be subtracted. We found that all these parameters for BMDCs stimulated with micelles were not different from the control cells, while stimulation with LPS led to decreased ATP turnover and decreased respiratory capacity (Figure 6B).

PBC Micelles Do Not Induce Detrimental ROS and NO Production by APCs.— Upon encounter with a pathogen or MAMPs, cells of the innate immune system induce the production of antimicrobial innate effector molecules.[48,49] These largely consist of various types of reactive oxygen and reactive nitrogen species. Since little to no upregulation of costimulatory molecules or increases in pro-inflammatory cytokine secretion was exhibited in response to the PBC micelles, we sought to determine if there was induction of ROS and NO in APCs upon encounter with the micelles. NO production was quantified from supernatants collected from BMDCs stimulated with micelle, LPS, or unstimulated controls and quantified via Griess assay. After 48 h of stimulation, LPS stimulation resulted in a marked accumulation of nitrite in the supernatants, while PBC micelle stimulation resulted in no accumulation of nitrite (Figure 7A). Similar results were observed in BMMs and J774 stimulations (SI Figure 5). BMDCs were also analyzed for mitochondrial superoxide and cytosolic ROS production. Similar patterns were observed in that LPS induced the production of large amounts of both superoxide and cytosolic ROS, while stimulation with PBC micelles resulted in no measurable increase in the production of these molecules (Figure 7B,C).

Discussion.

Adjuvants have played a major role in enhancing vaccine efficacy.[1,21,50] The mechanisms of action of adjuvants range from creating a depot, induction of inflammation, controlled release of antigen, and acting as DAMPs. There has been a significant amount of research on synthesizing new adjuvants, understanding their mechanism(s) of action, and improving them for different applications.[51] There are multiple viewpoints on the desirable characteristics of next-generation vaccine adjuvants.[51–53] There is a need to design new adjuvants and understand and exploit their immunomodulatory properties to specifically suit certain types of host immune systems, such as those of older adults and immunocompromised patients.

In this work, we showed that amphiphilic PBC micelle-based adjuvants can act as effective carriers for enhanced delivery of antigens to APCs and induce robust adaptive immunity without the production of NO and superoxides linked to the generation of an overt inflammation. Hydrogels formed by PDEAEM and Pluronic F127-based PBCs have been previously demonstrated to induce robust antibody responses as vaccine adjuvants and vaccines formulated with these materials effectively protected animals against viral challenge.[29,54] In the present work, we demonstrated that immunizing animals (C57BL/6 mice) with PBC micelles, at a significantly lower polymer concentration than previously reported,[55] enhanced anti-Ova antibody titers in mice (Figure 1) when compared with sOva alone. Though the antibody titers were still significant at 4 weeks p.i. compared with sOva alone, we observed a slight decrease in titers from 2 weeks to 4 weeks p.i. Our hypothesis is that the antigen-containing micelles may facilitate cross-linking the B cell receptor (BCR) and provide a rapid and low affinity antibody response.[56,57] This may be beneficial for presentation of the antigen or a coadjuvant to the receptors of immune cells in orientations exposing certain conformational epitopes of the antigen to cross-link multiple BCRs and provide an initial high burst of antigen, resulting in rapid induction of antibody; however, another adjuvant in combination with the micelles may

be required for induction of robust long-lasting immunity.[58] We also observed similar trends in enhancement of humoral immunity and improved vaccine efficacy with influenza antigens 2 and 4 weeks p.i. for PBC micelles alone and in combination with another vaccine adjuvant, polyanhydride nanoparticles.[54] We repeated the experiment with Ova adjuvanted with micelles administered to BALB/c mice and observed a similar enhancement in antibody responses (data not shown).

From previous studies, we had concluded that both the depot effect formed by hydrogels and the outer cationic blocks of the polymer contributed to enhanced antibody titers.[55] Since the PBC micelle concentration used in the present studies do not form a depot at the injection site, unlike the hydrogels, we hypothesize that the observed enhancement in humoral immunity may be attributed to the association of the antigen and the PBC micelles. There is significant interest in designing vaccine carriers to enhance cytosolic uptake of antigens resulting in enhanced presentation via the MHC I pathway and induction of $CD8^+$ T cell responses.[53,59] In this context, pH-responsive polycationic gene delivery systems, such as the PBC micelles, are known to translocate DNA from the endosome to the cytosol by induction of the endosomal escape of associated gene using a proton sponge effect.[15,60] Hence, we studied if these micelles associate with the antigens in a similar manner and deliver them to the cytosol.

We observed intracellular localization of the micelles and the associated ovalbumin into the cytosol of both BMDCs and J774 cells starting at an incubation period of 30 min and lasting until 12 h (Figure 2, SI Figure 1 and 2). Ova is known to be internalized after 15 min of incubation with APCs.[61] However, we did not observe a significant amount of internalization by the cells incubated with PBC micelles plus Ova in the first 15 min in either BMDCs or J774 cells (SI Figure 2 and 3). Other studies have shown that subsequently increasing amounts of Ova are detected after 15 min in the cytosol due to endosomal escape caused by the association with the carrier.[17] We showed association of Ova with the PBC micelles by FRET, in which energy transfer between fluorophores takes place in a nonradiative manner when they are separated by a distance referred to as the Forster radius for the two dyes (8.5 nm for our fluorophore system).[62–64] We observed the transfer of energy from donor to acceptor using the spectral emission curve at specific concentrations of the antigen and the micelles in solution (Figure 3). A similar technique was utilized previously for studying complexation of DNA with the PBC micelles.[37,65] We utilized the same concentrations for studying FRET in vitro with APCs using sensitized emission and a confocal microscope. Even though we did not calculate the numerical value of FRET efficiency, the FRET index image demonstrated the degree of FRET occurring quantitatively. The areas of strong association of the micelles with Ova as indicated by the FRET index image (Figure 4) within the cytosol indicated that the micelles transported the antigen to the cytosol. This hypothesis was supported by the FACS analysis, which quantitatively demonstrated enhanced uptake of Ova by BMDCs when associated with micelles rather than when delivered alone. Starting at 60 min of incubation with cells, the amount of Ova internalized steadily increased over 12 h of incubation. (Figure 4C and SI Figure 3). It is also worthwhile to note that we observed both stronger association of micelles with Ova and enhanced uptake of Ova in BMDCs than in J774 cells. The micelles appeared to be localized more around the cell membranes of the cells. Some studies have

demonstrated that amphiphilic molecules such as Pluronic can incorporate themselves into the lipid bilayer of the membranes and facilitate protein transport across it.[66,67]

All these observations have particular relevance to the rational design of vaccine formulations for older adults and immunocompromised populations. The current strategy in commercial vaccines for older adults (e.g., high dose Fluzone) is to deliver four times the amount of vaccine dose as the normal dose. In this context, the ability of the PBC micelles to increase the overall antigen internalization can be beneficial for vaccine delivery in older adults.[68]

Many adjuvants or immune potentiators, including the licensed adjuvant MPLA, act via the engagement of various receptors on innate immune cells and their stimulation, which can be measured by the upregulation of cell surface marker expression and cytokine secretion.[69] However, for PBC micelles, as demonstrated in Figure 5 and SI Figure 2, we did not observe any significant upregulation of these markers. Therefore, it appears that these micelles do not act as traditional immune stimulants or innate immune cell activators, such as TLR ligands. Indeed, the activation of APCs through TLRs may not always be desirable, especially when TLR agonists induce excessive NO production, which can cause cellular stress and contribute to acute inflammatory state of the immune system.[49,70,71] Higher amounts of NO production by inflammatory immune cells has been linked to lower B cell activation, diminished antibody responses, lower class-switching, and generation of more short-lived plasma cells then long-lived plasma cells.[10,72] In contrast, administration of PBC micelles did not lead to the production of NO or any cellular or mitochondrial ROS (Figure 7 and SI Figure 3) while still enhancing antibody production (Figure 1).

Finally, an analysis of the metabolic profile of APCs stimulated with the PBC micelles demonstrated low mitochondrial stress when compared with LPS (Figure 6). Rapid glycolytic activity as demonstrated by the TLR agonists in extracellular flux analysis has been reported to contribute to inflammation.[73] In a separate study using cathepsin activity, we have demonstrated that micelles do not induce inflammation at the site of injection.[31] Combined with the glycolytic activity of the micelles demonstrated in this work (Figure 6), this suggests that a potential benefit of micelle adjuvants would be to avoid adverse inflammatory reactions.

Overall, all these findings demonstrate that these PBC micelles, while not activating APCs in a way that traditional TLR agonists do, can still act as effective adjuvants for enhancing antibody responses in the context of low inflammation and increasing antigen trafficking into the cytosol of APCs. Given the enhanced intracellular localization of antigen in the presence of the PBC micelles, this observation is likely beneficial for designing an effective vaccine regimen to enhance host immune responses that have impaired APC functionality due to underlying inflammation and potentially to induce cytotoxic T cell responses.

CONCLUSIONS

In this work, we demonstrated that a low concentration of an amphiphilic pentablock copolymer that undergoes pH-sensitive micellization in aqueous solution can enhance

adaptive immune responses in mice without forming a gel depot. We showed that the PBC micelles associate with antigens and deliver them to the cytosol of APCs. We also demonstrated that these PBC micelles are different from traditional TLR agonists in terms of their activation of APCs as evidenced by the lack of costimulatory molecule expression, cytokine secretion, induction of NO and ROS, and immunometabolic profiles. Therein, we found that PBC micelle-based nanoadjuvants do not generate mitochondrial stress and do not create a harmful inflammatory environment. These attributes make the PBC micelle adjuvants attractive candidates in the design of vaccines for older adults and immunocompromised patients.

Supplementary Material

Refer to Web version on PubMed Central for supplementary material.

ACKNOWLEDGMENTS

The authors acknowledge funding from the National Institutes of Health (R01 AI127565-01 and R01 AI141196-01) and the Iowa State University Nanovaccine Institute. Surya Mallapragada and Balaji Narasimhan are grateful to the Carol Vohs Johnson Chair and the Vlasta Klima Balloun Faculty Chair, respectively.

REFERENCES

(1). Mallapragada SK; Narasimhan B Immunomodulatory biomaterials. Int. J. Pharm 2008, 364 (2), 265–271. [PubMed: 18662761]

(2). Vartak A; Sucheck SJ Recent Advances in Subunit Vaccine Carriers. Vaccines 2016, 4 (2), 12 DOI: 10.3390/vaccines4020012.

(3). Kurella S; Manocha M; Sabhnani L; Thomas B; Rao DN New age adjuvants and delivery systems for subunit vaccines. Indian J. Clin. Biochem 2000, 15 (S1), 83–100.

(4). Christensen D Vaccine adjuvants: Why and how. Hum. Vaccines Immunother 2016, 12 (10), 2709–2711.

(5). Reed SG; Orr MT; Fox CB Key roles of adjuvants in modern vaccines. Nat. Med 2013, 19 (12), 1597–1608. [PubMed: 24309663]

(6). Seder R; Reed SG; O'Hagan D; Malyala P; D'Oro U; Laera D; Abrignani S; Cerundolo V; Steinman L; Bertholet S Gaps in knowledge and prospects for research of adjuvanted vaccines. Vaccine 2015, 33, B40. [PubMed: 26022566]

(7). Lee Y-T; Kim K-H; Ko E; Lee Y-N; Kim M-C; Kwon Y-M; Tang Y; Cho M-K; Lee Y-J; Kang S-M New vaccines against influenza virus. Clin. Exp. Vaccine Res 2014, 3 (1), 12–28. [PubMed: 24427759]

(8). Haynes L; Swain SL Commentary Why Aging T Cells Fail: Implications for Vaccination. Immunity 2006, 24, 663–666. [PubMed: 16782020]

(9). Fulop T; Larbi A; Dupuis G; et al. Immunosenescence and Inflamm-Aging As Two Sides of the Same Coin: Friends or Foes? Front. Immunol 2018, 8, 1960. [PubMed: 29375577]

(10). Giordano D; Draves KE; Li C; Hohl TM; Clark EA Nitric Oxide Regulates BAFF Expression and T Cell-Independent Antibody Responses. J. Immunol 2014, 193 (3), 1110–1120. [PubMed: 24951820]

(11). Hubbell JA; Thomas SN; Swartz MA Materials engineering for immunomodulation. Nature 2009, 462, 449. [PubMed: 19940915]

(12). Yewdell JW Designing CD8+ T Cell Vaccines: It's Not Rocket Science (Yet). Curr. Opin. Immunol 2010, 22 (3), 402–410. [PubMed: 20447814]

(13). Bawa P; Pillay V; Choonara YE; du Toit LC Stimuli-responsive polymers and their applications in drug delivery. Biomed. Mater 2009, 4 (2), 022001. [PubMed: 19261988]

(14). Park TG; Jeong JH; Kim SW Current status of polymeric gene delivery systems. Adv. Drug Delivery Rev 2006, 58 (4), 467–486.

(15). Foster S; Duvall CL; Crownover EF; Hoffman AS; Stayton PS Intracellular delivery of a protein antigen with an endosomal-releasting polymer enhances CD8 T-cell production and prophylactic vaccine efficacy. Bioconjugate Chem. 2010, 21, 2205–2212.

(16). Li Y-Y; Li L; Dong H-Q; Cai X-J; Ren T-B Mater. Sci. Eng., C 2013, 33, 2698.

(17). Flanary S; Hoffman AS; Stayton PS Antigen delivery with poly (propylacrylic acid) conjugation enhances MHC-1 presentation and T-Cell activation. Bioconjugate Chem 2009, 20 (2), 241–248.

(18). Wilson JT; Keller S; Manganiello MJ; et al. PH-responsive nanoparticle vaccines for dual-delivery of antigens and immunostimulatory oligonucleotides. ACS Nano 2013, 7 (5), 3912–3925. [PubMed: 23590591]

(19). Agarwal A; Unfer R; Mallapragada SK Novel cationic pentablock copolymers as non-viral vectors for gene therapy. J. Controlled Release 2005, 103 (1), 245–258.

(20). Vogel BM; Mallapragada SK Synthesis of novel biodegradable polyanhydrides containing aromatic and glycol functionality for tailoring of hydrophilicity in controlled drug delivery devices. Biomaterials 2005, 26 (7), 721–728. [PubMed: 15350776]

(21). Adams JR; Mallapragada SK Enhancing the immune response through next generation polymeric vaccine adjuvants. Technology 2014, 02, 1–12.

(22). Determan MD; Cox JP; Seifert S; Thiyagarajan P; Mallapragada SK Synthesis and characterization of temperature and pH-responsive pentablock copolymers. Polymer 2005, 46, 6933–6946.

(23). Determan MD; Cox JP; Mallapragada SK Drug release from pH-responsive thermogelling pentablock copolymers. J. Biomed. Mater. Res., Part A 2007, 81A (2), 326–333.

(24). Sahay G; Alakhova DY; Kabanov AV Endocytosis of nanomedicines. J. Controlled Release 2010, 145 (3), 182–195.

(25). Iversen T-G; Skotland T; Sandvig K Endocytosis and intracellular transport of nanoparticles: Present knowledge and need for future studies. Nano Today 2011, 6 (2), 176–185.

(26). Phanse Y; Lueth P; Ramer-Tait AE; et al. Cellular internalization mechanisms of polyanhydride particles: Implications for rational design of drug delivery vehicles. J. Biomed. Nanotechnol 2016, 12 (7), 1544–1552. [PubMed: 29337493]

(27). Hillaireau H; Couvreur P Nanocarriers' entry into the cell: relevance to drug delivery. Cell. Mol. Life Sci 2009, 66 (17), 2873–2896. [PubMed: 19499185]

(28). Adams JR; Goswami M; Pohl NLB; Mallapragada SK Synthesis and functionalization of virus-mimicking cationic block copolymers with pathogen-associated carbohydrates as potential vaccine adjuvants. RSC Adv. 2014, 4 (30), 15655.

(29). Adams JR; Haughney SL; Mallapragada SK Acta Biomaterialia Effective polymer adjuvants for sustained delivery of protein subunit vaccines. Acta Biomater. 2015, 14, 104–114. [PubMed: 25484331]

(30). Ross K; Adams J; Loyd H; et al. Combination Nanovaccine Demonstrates Synergistic Enhancement in Efficacy against Influenza. ACS Biomater. Sci. Eng 2016, 2 (3), 368–374. [PubMed: 33429541]

(31). Adams JR; Senapati S; Haughney SL; Wannemuehler MJ; SM BN Safety and biocompatibility of injectible vaccine adjuvants composed of thermogelling block copolymer gels. Submitted to J. Biomed Mater. Res 2018

(32). Adams JR; Mallapragada SK Novel Atom Transfer Radical Polymerization Method to Yield Copper-Free Block Copolymeric Biomaterials. Macromol. Chem. Phys 2013, 214 (12), 1321–1325.

(33). Petersen LK; Xue L; Wannemuehler MJ; Rajan K; Narasimhan B The simultaneous effect of polymer chemistry and device geometry on the in vitro activation of murine dendritic cells. Biomaterials 2009, 30 (28), 5131–5142. [PubMed: 19539989]

(34). Hachet-Haas MH; Converset N; Marchal O; Matthes H; Gioria S; Galzi JL; Lecat S FRET and Colocalization Analyzer— A Method to ValidateMeasurements of Sensitized Emission FRET Acquired byConfocal Microscopy and Available as an ImageJ Plug-in. Microsc. Res. Tech 2006, 69, 941–956. [PubMed: 17080432]

(35). Arsov Z; Švajger U; Mravljak J; et al. Internalization and Accumulation in Dendritic Cells of a Small pH-Activatable Glycomimetic Fluorescent Probe as Revealed by Spectral Detection. ChemBioChem 2015, 16 (18), 2660–2667. [PubMed: 26515511]

(36). Tomić S; Đokić J; Vasilijić S Size-Dependent Effects of Gold Nanoparticles Uptake on Maturation and Antitumor Functions of Human Dendritic Cells In Vitro. PLoS One 2014, 9 (5), e96584. [PubMed: 24802102]

(37). Jia F; Zhang Y; Narasimhan B; Mallapragada SK Block copolymer-quantum dot micelles for multienzyme colocalization. Langmuir 2012, 28 (50), 17389–17395. [PubMed: 23171402]

(38). Bobryshev YV; Karagodin VP; Orekhov AN Dendritic cells and their role in immune reactions of atherosclerosis. Cell tissue biol. 2013, 7 (2), 113–125.

(39). van Vliet SJ; García-Vallejo JJ; van Kooyk Y Dendritic cells and C-type lectin receptors: coupling innate to adaptive immune responses. Immunol. Cell Biol 2008, 86 (7), 580–587. [PubMed: 18679407]

(40). Petersen LK; Ramer-Tait AE; Broderick SR; et al. Activation of innate immune responses in a pathogen-mimicking manner by amphiphilic polyanhydride nanoparticle adjuvants. Biomaterials 2011, 32 (28), 6815–6822. [PubMed: 21703679]

(41). Thwe PM; Amiel E The role of nitric oxide in metabolic regulation of Dendritic cell immune function. Cancer Lett. 2018, 412, 236–242. [PubMed: 29107106]

(42). Everts B; Pearce EJ Metabolic control of dendritic cell activation and function: Recent advances and clinical implications. Front. Immunol 2014, 5, 203. [PubMed: 24847328]

(43). O'Neill LAJ; Pearce EJ Immunometabolism governs dendritic cell and macrophage function. J. Exp. Med 2016, 213 (1), 15–23. [PubMed: 26694970]

(44). Krawczyk CM; Holowka T; Sun J; et al. Toll-like receptor-induced changes in glycolytic metabolism regulate dendritic cell activation. Blood 2010, 115 (23), 4742–4749. [PubMed: 20351312]

(45). Everts B; Amiel E; Van Der Windt GJW; et al. Commitment to glycolysis sustains survival of NO-producing inflammatory dendritic cells. Blood 2012, 120 (7), 1422–1431. [PubMed: 22786879]

(46). Everts B; Amiel E; Huang SCC; et al. TLR-driven early glycolytic reprogramming via the kinases TBK1-IKKε supports the anabolic demands of dendritic cell activation. Nat. Immunol 2014, 15 (4), 323–332. [PubMed: 24562310]

(47). Kanof ME Isolation of T Cells Using Rosetting Procedures 2016, 1–5.

(48). Serbina NV; Salazar-Mather TP; Biron CA; Kuziel WA; Pamer EG TNF/iNOS-producing dendritic cells mediate innate immune defense against bacterial infection. Immunity 2003, 19 (1), 59–70. [PubMed: 12871639]

(49). Bogdan C Nitric oxide synthase in innate and adaptive immunity: An update. Trends Immunol. 2015, 36 (3), 161–178. [PubMed: 25687683]

(50). Wilson-Welder JH; Torres MP; Kipper MJ; Mallapragada SK; Wannemuehler MJ; Narasimhan B Vaccine adjuvants: Current challenges and future approaches. J. Pharm. Sci 2009, 98 (4), 1278–1316. [PubMed: 18704954]

(51). Brito LA; O'Hagan DT Designing and building the next generation of improved vaccine adjuvants. J. Controlled Release 2014, 190, 563–579.

(52). Narasimhan B; Goodman JT; Vela Ramirez JE Rational Design of Targeted Next-Generation Carriers for Drug and Vaccine Delivery. Annu. Rev. Biomed. Eng 2016, 18, 25. [PubMed: 26789697]

(53). O'Hagan DT; Fox CB New generation adjuvants - From empiricism to rational design. Vaccine 2015, 33 (S2), B14–B20. [PubMed: 26022561]

(54). Ross K; Adams J; Loyd H; et al. Combination Nanovaccine Demonstrates Synergistic Enhancement in Efficacy against Influenza. ACS Biomater. Sci. Eng 2016, 2 (3), 368–374. [PubMed: 33429541]

(55). Adams JR; Haughney SL; Mallapragada SK Effective polymer adjuvants for sustained delivery of protein subunit vaccines. Acta Biomater. 2015, 14, 104–114. [PubMed: 25484331]

(56). Hitomi T; Yanagi S; Inatome R; Yamamura H Cross-linking of the B cell receptor induces activation of phospholipase D through Syk, Btk and phospholipase C-γ2. FEBS Lett. 1999, 445 (2–3), 371–374. [PubMed: 10094492]

(57). Liu W; Sohn HW; Tolar P; Pierce SK It's all about change: the antigen-driven initiation of B-cell receptor signaling. Cold Spring Harbor Perspect. Biol 2010, 2 (7), a002295.

(58). Ross K; Senapati S; Alley J; et al. Single dose combination nanovaccine provides protection against influenza A virus in young and aged mice. Biomater. Sci 2019, DOI: 10.1039/C8BM01443D.

(59). Zacharias ZR; Ross KA; Hornick EE; et al. Polyanhydride Nanovaccine Induces Robust Pulmonary B and T Cell Immunity and Confers Protection Against Homologous and Heterologous Influenza A Virus Infections. Front. Immunol 2018, 9, 1953. [PubMed: 30233573]

(60). Cho YW; Kim J-D; Park K Polycation gene delivery systems: escapes from endosome to cytosol. J. Pharm. Pharmacol 2003, 55, 721–734. [PubMed: 12841931]

(61). Platt CD; Ma JK; Chalouni C; et al. Mature dendritic cells use endocytic receptors to capture and present antigens. Proc. Natl. Acad. Sci. U. S. A 2010, 107 (9), 4287–4292. [PubMed: 20142498]

(62). Gravier J; Sancey L; Hirsjärvi S; et al. FRET imaging approaches for in vitro and in vivo characterization of synthetic lipid nanoparticles. Mol. Pharmaceutics 2014, 11 (9), 3133–3144.

(63). Sekar RB; Periasamy A Fluorescence resonance energy transfer (FRET) microscopy imaging of live cell protein localizations. J. Cell Biol 2003, 160 (5), 629–633. [PubMed: 12615908]

(64). Morton SW; Zhao X; Quadir MA; Hammond PT Biomaterials FRET-enabled biological characterization of polymeric micelles. Biomaterials 2014, 35 (11), 3489–3496. [PubMed: 24477190]

(65). Zhang B; Zhang Y; Mallapragada SK; Clapp AR ACS Nano 2011, 5 (1), 129–138. [PubMed: 21190373]

(66). Gaurav S; Elena VB; Alexander VK Different internalization pathways of polymeric micelles and unimers and their effects on vesicular transport. Bioconjug Chem. 2008, 19 (10), 2023–2029. [PubMed: 18729494]

(67). Kabanov AV; Levashov AV; Alakhov VY Lipid modification of proteins and their membrane transport. Protein Eng., Des. Sel 1989, 3 (1), 39–42.

(68). Centers for Disease Control and Prevention. Fluzone High-Dose Seasonal Influenza Vaccine. https://www.cdc.gov/flu/protect/vaccine/qa_fluzone.htm.

(69). Flower DR Systematic identification of small molecule adjuvants. Expert Opin. Drug Discovery 2012, 7 (9), 807–817.

(70). Sun J; Zhang X; Broderick M; et al. Measurement of Nitric Oxide Production in Biological Systems by Using Griess Reaction Assay. Sensors 2003, 3 (8), 276–284.

(71). Stuehr DJ; Marletta MA Mammalian nitrate biosynthesis: mouse macrophages produce nitrite and nitrate in response to Escherichia coli lipopolysaccharide. Proc. Natl. Acad. Sci. U. S. A 1985, 82 (22), 7738–7742. [PubMed: 3906650]

(72). Sammicheli S; Kuka M; Di Lucia P; et al. Inflammatory monocytes hinder antiviral B cell responses. Sci. Immunol 2016, 1 (4), eaah6789. [PubMed: 27868108]

(73). Pence BD; Yarbro JR Aging impairs mitochondrial respiratory capacity in classical monocytes. Exp. Gerontol 2018, 108, 112–117. [PubMed: 29655929]

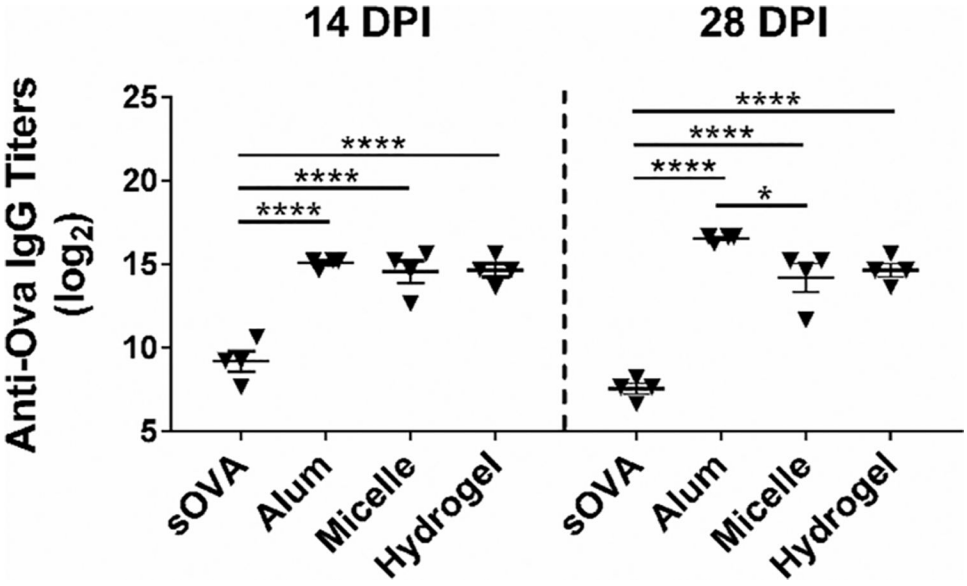

Figure 1.

Pentablock copolymer (PBC) micelles enhanced antibody titers in C57BL/6 mice 2- and 4-weeks postimmunization. Serum collected at 14 and 28 dpi were used to evaluate anti-OVA total IgG titers using ELISA. Statistical differences between the treatment groups within each time-point were determined using one-way ANOVA and Tukey-post *t* test on the log 2 transforms of the titer dilution values. * indicates $p < 0.05$ and **** indicates $p < 0.0001$. Data are representative of two independent experiments with C57BL/6 mice and one independent experiment with BALB/c mice with 4–5 animals in each experiment per treatment group.

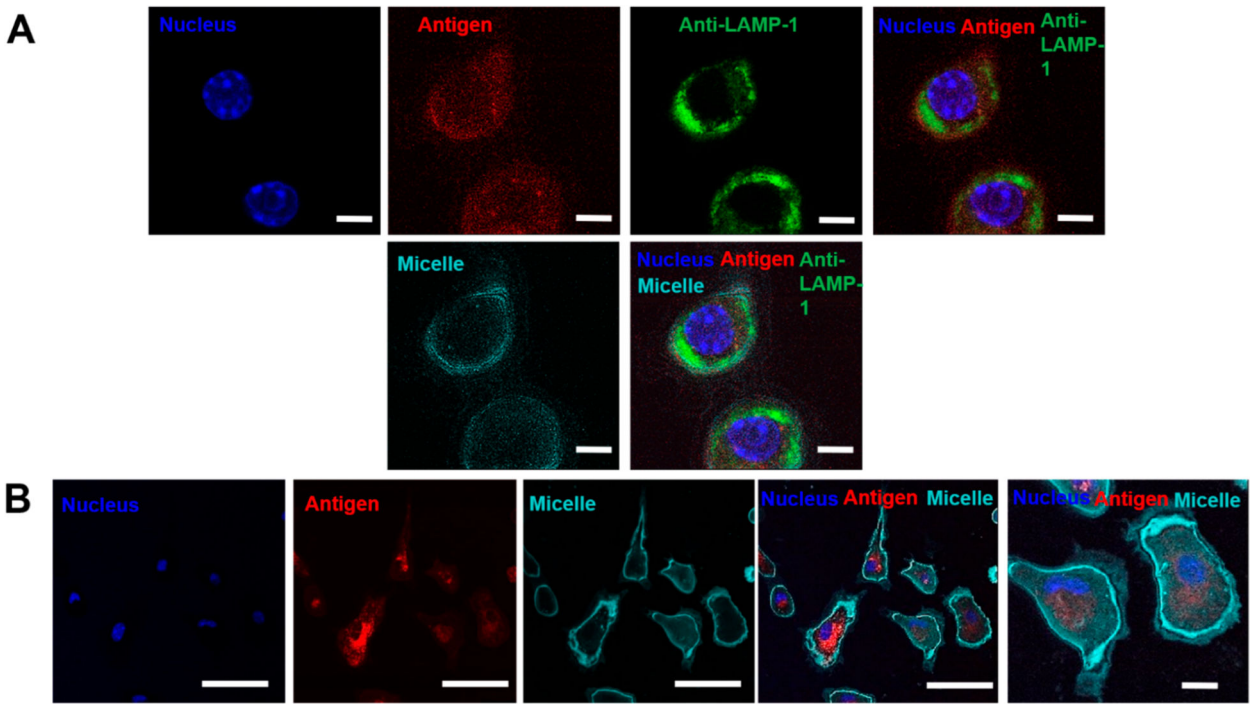

Figure 2.

Pentablock copolymer (PBC) micelles efficiently traffic antigen to the cytosol. (A) Bone marrow derived dendritic cells (BMDCs) and (B) J774 cells were incubated with micelles and ovalbumin (i.e., antigen) for 12 h over glass coverslips. Cell components were stained following the incubation and cells were fixed and transferred to glass slides for imaging. Scale bars indicate 5 μm in A and 50 and 5 μm in the first four and last columns of B, respectively. Nuclei were stained with Hoescht (blue), lysosomes were stained with anti-LAMP-1 (green). Ovalbumin antigen (AF594) and PBC micelles (AF647) are denoted by red and cyan, respectively. Data are representative of four independent experiments.

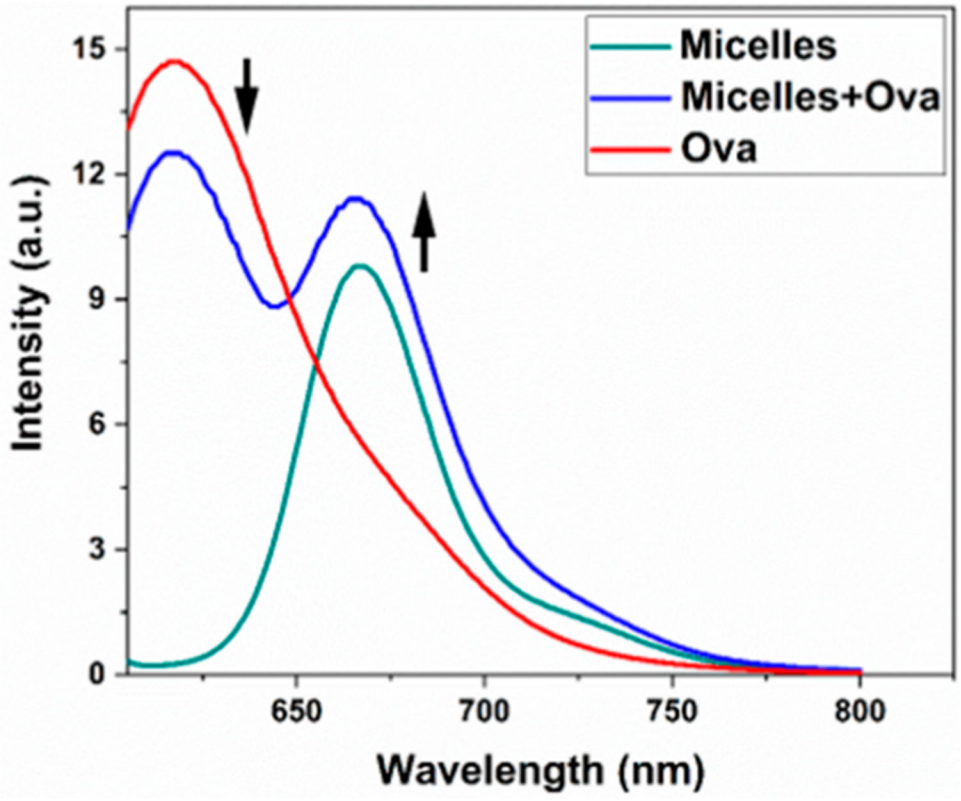

Figure 3.

Pentablock copolymer (PBC) micelles associated with ovalbumin in solution phase. Micelles (12.5 mg/mL) and ovalbumin (20 mg/mL) were labeled with AF647 and AF594, respectively. The fluorescence spectra were measured for micelles only, ovalbumin only, and micelles plus ovalbumin mixtures. Arrows indicate decrease in AF594 (donor) fluorescence and increase in AF647 (acceptor) fluorescence.

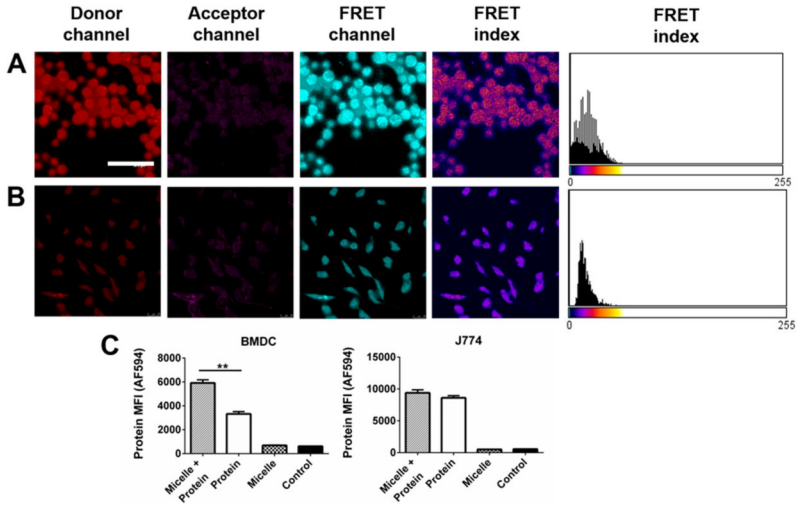

Figure 4.

Pentablock copolymer (PBC) micelles associated with ovalbumin intracellularly and enhanced the uptake of ovalbumin in BMDCs. FRET microscopic analysis of (A) BMDCs and (B) J774 cells demonstrated strong association of micelles with protein with FRET indices of 16.8 and 9.6, respectively. Histograms in the far right represent the mean FRET indices with the heat map for the “fire” Look-Up Table (LUT) used in the FRET index images. Excitation and emission wavelengths (Ex/Em) used to image are Donor channel: 590 nm/620 nm, Acceptor channel: 650 nm/665 nm and FRET channel: 590 nm/665 nm. (C) Ovalbumin uptake was increased 2-fold when delivered with micelles in BMDCs. Statistical significance was determined using unpaired *t* test. ** indicates $p < 0.002$.

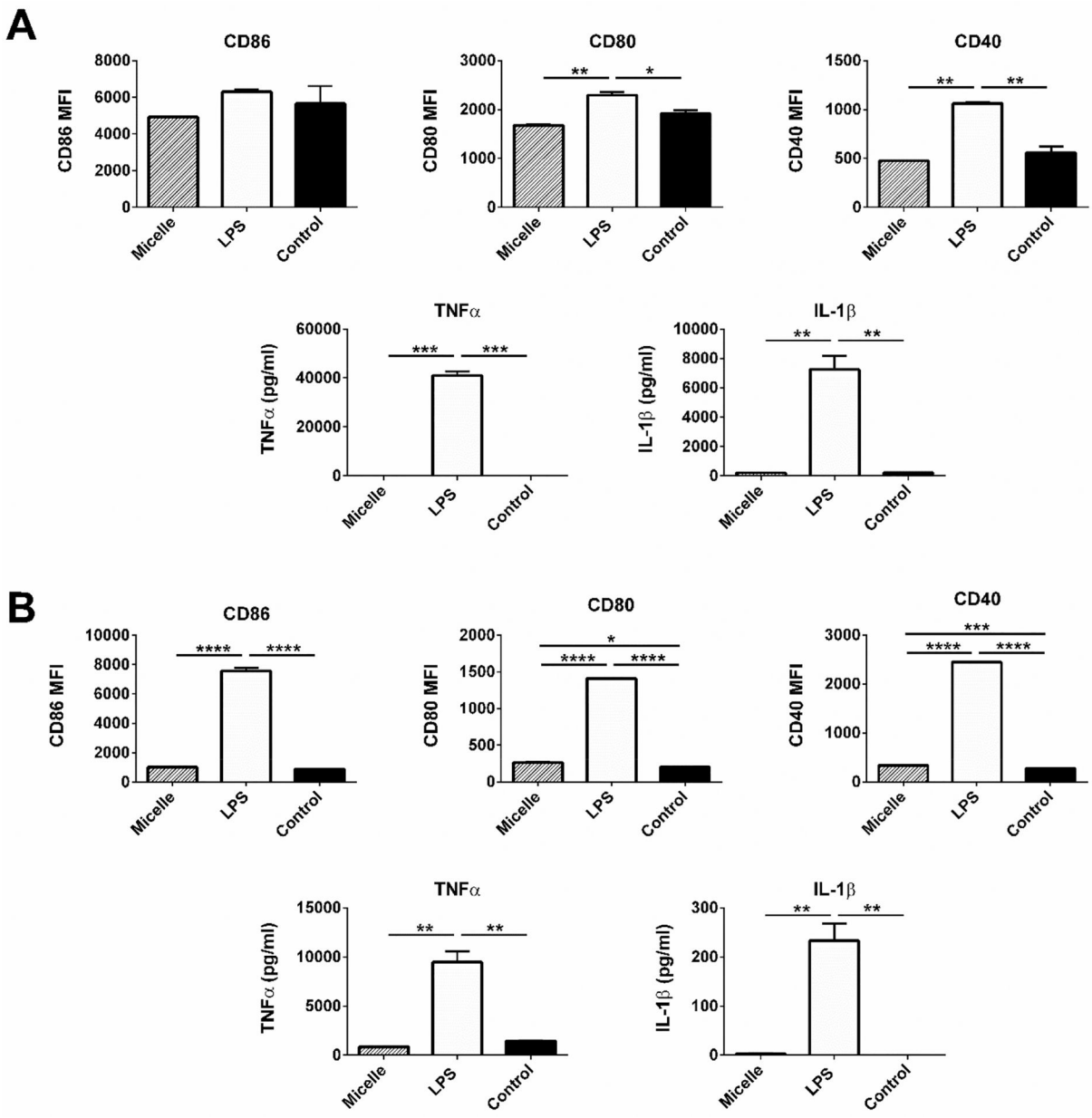

Figure 5.

Pentablock copolymer (PBC) micelles did not activate innate immune cells as exhibited by cell surface markers expression and less inflammatory cytokines secretions. (A) BALB/c-derived BMDCs and (B) J774 cells at a concentration of 2.5×10^6 cells/mL were stimulated with different treatment groups (PBC micelles at the concentration of 12.5 μg/mL and LPS at 1 μg/mL) for 48 h. Flow cytometry was used to measure the cell surface marker upregulation. Cytokine secretion was evaluated from the supernatants collected after stimulation. Data is expressed as mean with standard error of mean. Statistical differences were determined using one-way ANOVA. *indicates $p < 0.05$, ** indicates $p < 0.005$ and *** indicates $p < 0.0005$.

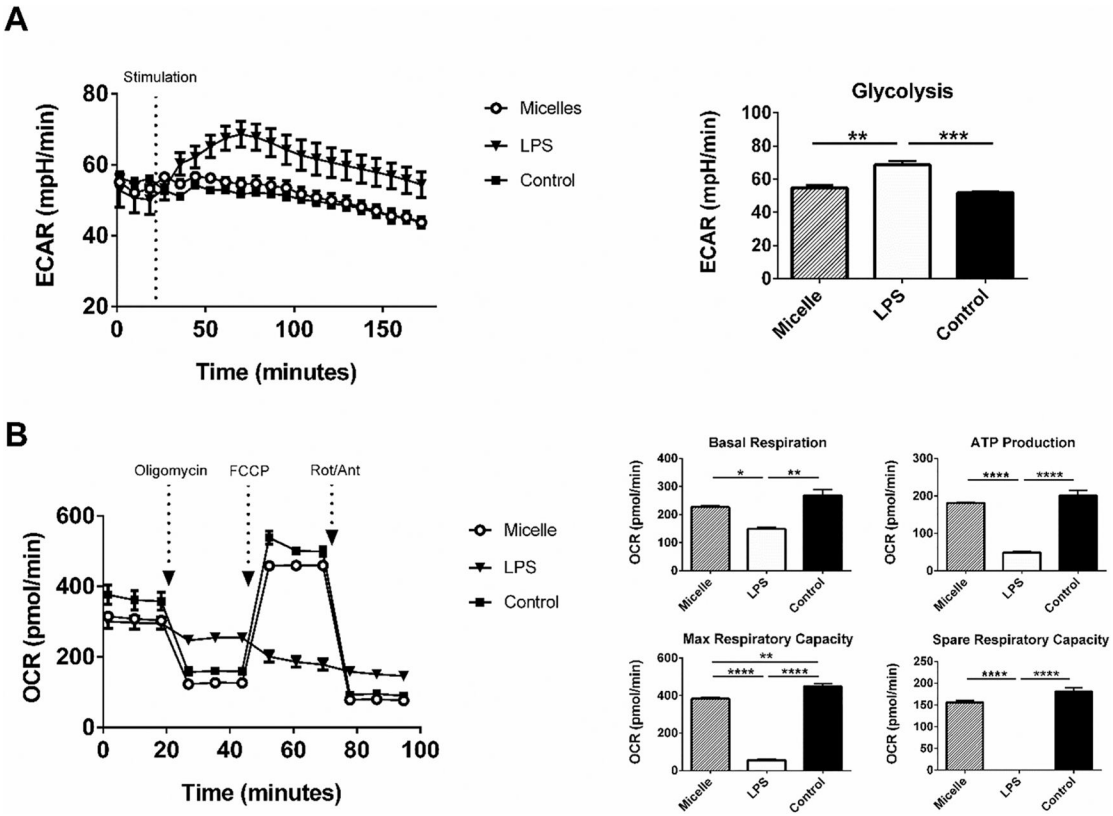

Figure 6.

Treatment of BMDCs with pentablock copolymer (PBC) micelles did not induce a glycolytic shift in their metabolic profile. (A) Kinetic stimulation test and (B) Mitochondrial stress test for BMDCs stimulated with different treatment groups (PBC micelles at the concentration of 12.5 μg/mL and LPS at 1 μg/mL) was performed overnight using extracellular flux analysis. Extracellular acidification rate (ECAR) and oxygen consumption rate (OCR) are represented by millipH/min and pmol/min. The figure on top right represents ECAR value at 61 min and figures in the bottom right represent different measures of the mitochondrial respiration derived from B as indicated in the text using standard methods. * indicates $p < 0.02$, ** indicates $p < 0.002$ and *** indicates $p < 0.0002$. $n = 2$.

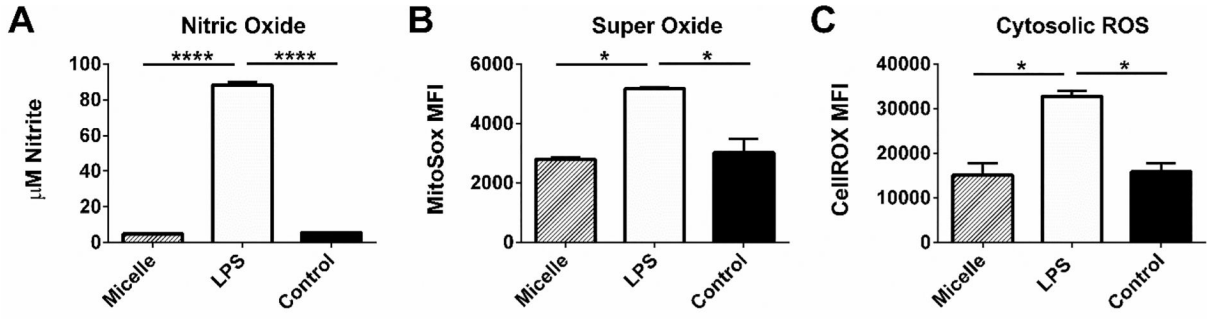

Figure 7.

Pentablock copolymer (PBC) micelle adjuvants did not induce the production of NO or ROS by APCs. (A) Nitric oxide production by BMDCs, (B) BMDC mitochondrial superoxide production, and (C) reactive oxygen species production in the BMDC cytosol were measured in the supernatants and cells stimulated with the treatment groups (PBC micelles at the concentration of 12.5 μg/mL and LPS at 1 μg/mL) for 48 h using Griess assay and flow cytometry. Data is expressed as mean with standard error of mean. Statistical differences were determined using one-way ANOVA. * indicates $p < 0.01$ and **** indicates $p < 0.0001$. $n = 3$.